Talanta 84 (2011) 160–168

Contents lists available at ScienceDirect

Talanta

journal homepage: www.elsevier.com/locate/talanta

Sensitive voltammetric determination of baicalein at DNA Langmuir–Blodgett film modified glassy carbon electrode

Fei Wang[a,b], Fangyuan Zhao[a], Yanzheng Zhang[a], Huige Yang[a], Baoxian Ye[a,*]

[a] Department of Chemistry, Zhengzhou University, Zhengzhou 450052, PR China
[b] Department of Material and Chemistry Engineering, Henan Institute of Engineering, Zhengzhou 450007, PR China

ARTICLE INFO

Article history:
Received 18 August 2010
Received in revised form
17 December 2010
Accepted 21 December 2010
Available online 8 January 2011

Keywords:
Baicalein
Square wave voltammetry
Langmuir–Blodgett film
DNA

ABSTRACT

The present paper describes to modify a double stranded DNA–octadecylamine (ODA) Langmuir–Blodgett film on a glassy carbon electrode (GCE) surface to develop a voltammetric sensor for the detection of trace amounts of baicalein. The electrode was characterized by atomic force microscopy (AFM) and cyclic voltammetry (CV). Electrochemical behaviour of baicalein at the modified electrode had been investigated in pH 2.87 Britton–Robinson buffer solutions by CV and square wave voltammetry (SWV). Compared with bare GCE, the electrode presented an electrocatalytic redox for baicalein. Under the optimum conditions, the modified electrode showed a linear voltammetric response for the baicalein within a concentration range of 1.0×10^{-8}–2.0×10^{-6} mol L^{-1}, and a value of 6.0×10^{-9} mol L^{-1} was calculated for the detection limit. And the modified electrode exhibited an excellent immunity from epinephrine, dopamine, glucose and ascorbic acid interference. The method was also applied successfully to detect baicalein in the medicinal tablets and spiked human blood serum samples with satisfactory results.

1. Introduction

Flavonoids have aroused an increasing awareness for their potential health a valuable effect [1]. Baicalein, a kind of flavonoid found in the root of *Scutellaria baicalensis*, has been widely used in traditional Chinese's medicine for a long time [2]. Fig. 1 shows its corresponding chemical structure. It has been reported to present anti-inflammatory [3], anti-HIV [4], anticancer [5–8], free radical scavenging and antioxidant effects [9,10]. Hence, the quantification of baicalein is of considerable interest. Some analytical methods, including UV–vis spectrophotometry [11], chemiluminescence [12], thin layer chromatography (TLC) [13], high performance liquid chromatography (HPLC) [14,15] and capillary electrophoresis (CE) [16,17] have been applied to determine baicalein. However, complicated preconcentrations, multisolvent extraction techniques or needs expensive devices and maintenance are coupled with these techniques. More inadequate, the pharmacological action and reaction mechanism of the medicine are not observed using these methods. Electrochemical methods offer improved characteristics such as short time, little reagent consumption, easy operation and environmental friendly. More importantly, the techniques also help for identifying the redox of drug compounds and provide important information about pharmacological actions.

There have been extensive researches on DNA-modified electrodes as an electrochemical sensor to small molecules [18–20]. Most of these sensors typically possess a single stranded (ss) DNA and are based on nucleic acid recognition towards the detection of genetic hybridization to the immobilized DNA on the electrodes [20–23]. Double stranded DNA (dsDNA) modified electrodes can also be used as sensitive sensors to small molecules that interact with DNA. The quantification of drugs or drug monitoring based on DNA–drug interactions has been reported [24–28]. But one of the most important problems in electrochemical DNA sensors is the model of immobilizing DNA onto electrode surfaces. Some research works are reported, such as adsorption [29], self-assembled immobilization [30] and covalent immobilization [20].

Langmuir–Blodgett (LB) technique offers a possibility of developing an ultra-thin film with well-ordered structure at the molecular level [31]. Nevertheless, loading of the amount of components can be controlled by the number of deposited layers. Thus, attempts have recently been made to fabricate LB films of organic and inorganic materials for sensor applications [32–34]. So far as we know, rare work has been reported yet on immobilizing dsDNA by LB technique to design a sensor. In the recent, we presented that DNA LB films were immobilized onto a glassy carbon electrode (GCE) surface as a voltammetric sensor for determination of methotrexate and 8-Azaguanine [25,26]. Here, DNA LB film was produced from spreading the octadecylamine (ODA) chloroform solution on aqueous DNA solutions with concentration of 3 μg mL^{-1}.

* Corresponding author. Tel.: +86 0371 67781757; fax: +86 0371 67763654.
E-mail address: yebx@zzu.edu.cn (B. Ye).

0039-9140/$ – see front matter © 2011 Elsevier B.V. All rights reserved.
doi:10.1016/j.talanta.2010.12.036

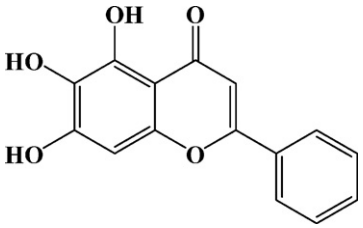

Fig. 1. The chemical structure of baicalein.

In this approach, to avoid DNA adsorption on the electrode surface before deposition, DNA–ODA LB film was formed by spreading DNA solution direct onto subphase covered with a layer of ODA. After well-distributed, a layer of DNA–ODA LB was transferred to GCE surface slowly and a designed DNA modified electrode was fabricated, named DNA-LB/GCE. A pair of well-defined redox peak of baicalein was noted at DNA-LB/GCE. The peak current, evaluated by using both cyclic voltammetry (CV) and square wave voltammetry (SWV) techniques, was about 20-fold higher at the DNA-LB/GCE than that got at bare GCE. In addition, the reductive peak currents of baicalein were linearly responding to the baicalein concentration in the range of 1.0×10^{-8}–2.0×10^{-6} mol L^{-1}, and the modified electrode was applied as a sensor to decide baicalein in medicinal tablets and spiked human blood serum samples with satisfactory results.

2. Experimental

2.1. Apparatus and reagents

Model 650A electrochemical system (CHI Instrument Company, Shanghai, China) was employed for electrochemical techniques. A standard three-electrode electrochemical cell was used for all electrochemical experiments with a bare GCE or modified electrode (d = 3 mm) as working electrode, a platinum (Pt) wire as an auxiliary electrode and a saturated calomel electrode (SCE) as a reference electrode. LB films were performed with a JML-04 LB trough (Shanghai Zhongchen Co., Shanghai, China). All the pH measurements were carried out with a pHS-2C Digital pH meter (Shanghai Lida, Shanghai, China) equipped with a combined glass electrode, which was calibrated regularly with standard buffer solutions (pH 4.00 and 6.86) at 25 ± 0.1 °C.

All reagents were of analytical grade and were used as received. Baicalein was purchased from National Institute for the Control of Pharmaceutical and Biological Products (Beijing, China), and Fish Sperm DNA were supplied by Shanghai Sangon Company (Shanghai, China). Double distilled water was used for all preparations. Stock solutions (5.0×10^{-4} mol L^{-1}) of baicalein were prepared with ethanol and stored at 4 °C darkly. Dilutions were done just before use. Fish Sperm DNA solution was prepared with doubly distilled water and renewed every day. Each assay was performed at room temperature.

2.2. Electrode pretreatment and DNA-modified procedure

The experiments were conducted at room temperature, approximately 25 °C. Prior to modification, the GCE was polished with finer emery paper and 0.1 μm alumina slurry to get a mirror surface, and successively rinsed thoroughly with acetone, ethanol, and distilled water in ultrasonic bath respectively, each for 1 min. And then, it was treated in 0.10 mol L^{-1} phosphate buffer solution (pH 5.0) by applying a potential of +1.75 V for 300 s under constant stirring. Finally, cyclic voltammetry was carried out in the same solution with a scan potential window of between 0.30 V and 1.25 V with a scan rate of 50 mV s^{-1}, until a stable CV profile was obtained [35].

A sample of ODA in a dichloromethane solution was spread onto the subphase (pure water) surface using a micro injector, allowing the solvent to evaporate for 30 min. Then, some of dsDNA was spread carefully using a micro injector onto the subphase's interface covered with a layer of ODA. When the equilibrium between DNA and ODA monolayer was established, the pressure–area (π–A) isotherm was recorded using the JML-04 trough with a compression rate of 10 mm min^{-1}. Under the surface pressure of 35.0 mN m^{-1}, a monolayer of DNA–ODA was transferred onto GCE surface with a rate of 2.5 mm min^{-1} (vertical dipping). Fig. 2 shows the scheme of DNA–ODA LB film forming on the air–water interface. The multilayer films were assembled by sequential monolayer transfer. Between two monolayer transfers, the electrode was dried at least 1 h in air. For comparison, an ODA modified electrode (without DNA) was fabricated by the same method, named ODA/GCE. Besides, 5 μL of 1 mg mL^{-1} DNA was directly casting on the GCE surface to make a DNA modified electrode, named DNA/GCE. All of these modified electrodes were thoroughly rinsed with pure water and stored in 0.01 mol L^{-1} phosphate buffer (pH = 7.0) at 4 °C when not in use.

2.3. Tablets assay procedure

The sample powder was obtained by grinding 5 Huanglian Shangqing tablets (Zhengzhou Yumi Pharmaceutical Co., Ltd.). Accurate amount of the powder was weighed and extracted with 50 mL ethanol for 30 min in an ultrasonic bath. The solution was filtered into a 100 mL volumetric flask through an ordinary filtration paper, and then the solution was diluted to the exact volume with ethanol. Sample solution was stored in the dark. Just before each measurement, the sample solution was diluted quantitatively using the supporting electrolyte.

2.4. Analysis of spiked serum samples

Serum samples of healthy individuals (after having obtained their written consent) were stored frozen until assay. Acetonitrile removes serum proteins more effectively, to add 1 volume of serum is enough to remove the proteins. The mixture was then centrifuged for 30 min at 5000 rpm for getting rid of serum protein residues and the supernatant was taken carefully. Suitable volumes of this supernatant were transferred into the volumetric flask and diluted up to the volume with distilled water. Sample solution was stored in the dark. Just before each measurement, the sample solution was diluted quantitatively using the supporting electrolyte.

3. Results and discussion

3.1. π–A isotherms of DNA LB films

Fig. 3 shows surface pressure (π) versus area (A) isotherms of pure ODA film and DNA–ODA film. On π–A isotherms of pure ODA film (Fig. 3, curve a), the monolayer of ODA gives a steep rise in surface pressure and the minimum area per molecule is obtained to be 0.22 nm^2. When some of DNA was spread carefully onto the subphase's interface covered with a layer of ODA, an increase of the initial surface pressure was observed (Fig. 3, curves b–d). This is the evidence of that DNA molecules entered ODA layer. This behaviour was attributed to electrostatic interaction between the negatively charged DNA and cationic ODA molecules incorporating DNA molecules into the ODA membrane at the air–water interface [36]. The equilibrium time of DNA molecules was estimated as 1 h

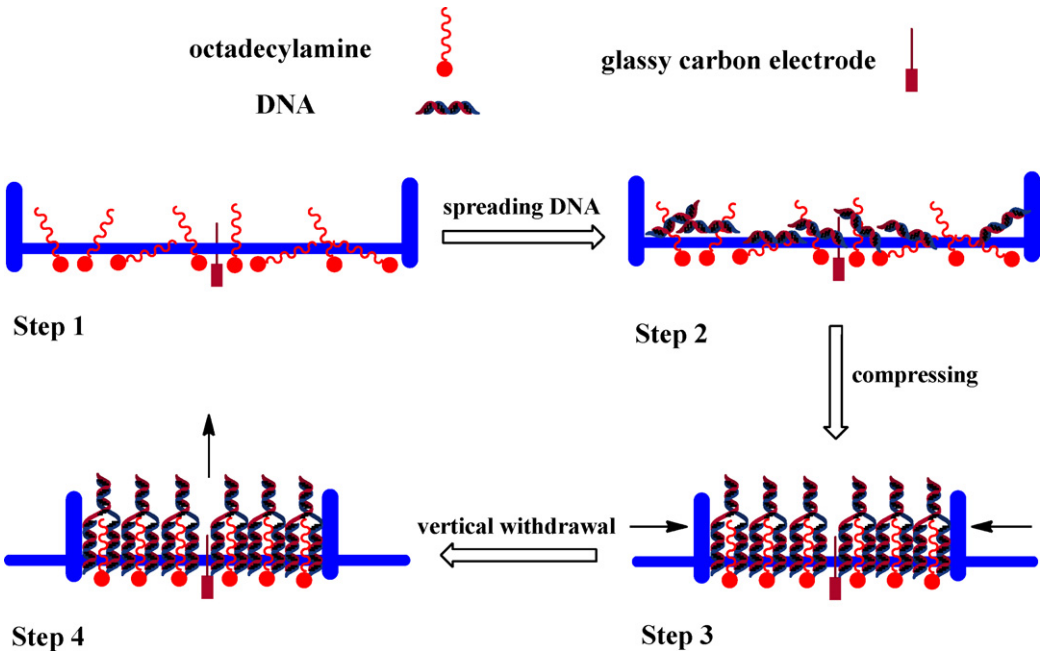

Fig. 2. Scheme of DNA LB film forming on air–water interface and deposition.

according to surface pressure. The π–A isotherms were recorded at a barrier speed of 10 mm min^{-1} and the curves b, c and d were obtained with DNA concentration of 1.5 μg mL^{-1}, 3.0 μg mL^{-1}, and 4.5 μg mL^{-1} respectively.

When surface pressure reached 35.0 mN m^{-1} or so, film area of DNA–ODA monolayer with different amounts of DNA was nearly the same, which meant that parts of DNA molecules were driven out during compressing process. The more DNA is added, the more the DNA molecules are expelled from mixed film. Thus, the same amount of DNA was incorporated in ODA layer finally. When the amount of DNA added was more than 3.0 μg mL^{-1}, compressibility curves of DNA–ODA complex layer had not significantly changed, indicating that DNA–ODA ratio of incorporation film was the same. Thus, the suitable amount of DNA was 3.0 μg mL^{-1}. At the same time, to obtain a compact and ordered DNA–ODA LB film on the electrode surface, the surface pressure of 35.0 mN m^{-1} was chosen to transfer the DNA–ODA LB film from air–water interface to the electrode surface by vertical withdrawal method. The withdrawal speed was 2.5 mm min^{-1}.

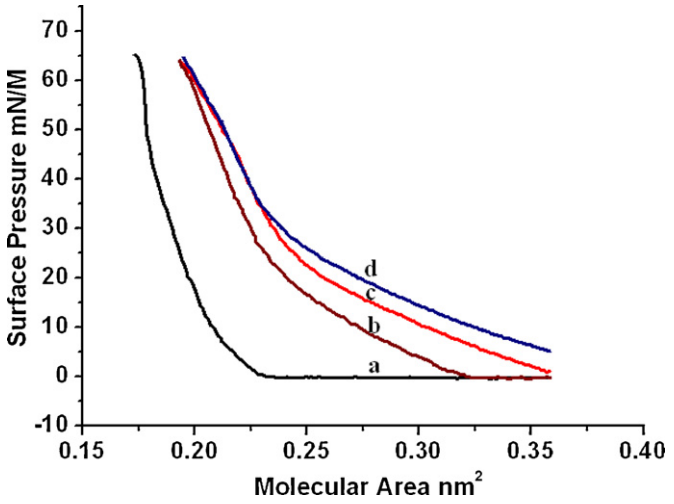

Fig. 3. π–A isotherms of ODA monolayer on pure water (curve a) and spreading different amounts of DNA onto subphase covered with a layer of ODA (curves b–d); curve b: 1.5 μg mL^{-1}, curve c: 3.0 μg mL^{-1}, curve d: 4.5 μg mL^{-1}.

3.2. Atomic force microscopy image of DNA–ODA LB films

Atomic force microscope (AFM) was employed to observe the structure of DNA–ODA LB films. Silicon was used as substrates to substitute GCE. Silicon substrates were sonicated successively in ethanol and redistilled water respectively, each for 10 min. Then the substrates were dipped in piranha solution (1:3 mixtures of H_2O_2 and H_2SO_4) for 20 min. Later, they were again ultrasonic cleaned in redistilled water for 5 min. Finally, the pretreated silicon was kept in redistilled water for further using. Fig. 4 shows the typical contact mode AFM images of the bare silicon surface and the silicon covered with a layer of DNA–ODA LB film that was transferred from air–water interface to the silicon surface under the surface pressure of 35.0 mN m^{-1}. The bare silicon has no impurity on its surface and shows very even surface (Fig. 4A). The compact and well-ordered structure of DNA–ODA LB film was observed (Fig. 4B) which was formed by aggregates of DNA molecules during compressing process. These data indicate the DNA–ODA film was successfully immobilized on the substrate surface just as design.

3.3. Cyclic voltammetry characterization of the DNA-LB/GCE

To provide further information about the electrochemical properties of DNA-LB/GCE, potassium ferricyanide was selected as a probe to evaluate the performance of the fabricated electrodes. Fig. 5 showed electrochemical responses of the bare GCE, the ODA/GCE and different layer of DNA-LB/GCE in 2.0×10^{-3} mol L^{-1} $K_3[Fe(CN)_6]$ + 0.2 mol L^{-1} KCl solution, respectively. Well-defined CV, characteristic of a diffusion-limited and reversible electron transfer redox process, was observed at the bare GCE (Fig. 5, curve a). Using the ODA/GCE, the redox peak currents decreased and the peak potential separation increased slightly (Fig. 5, curve b). When DNA–ODA LB films was modified on the electrode, the redox peak currents decreased and the peak potential separation increased remarkably by increasing the modified layer (Fig. 5, curves c–e). The result indicated that the negative probe is difficult to pass through

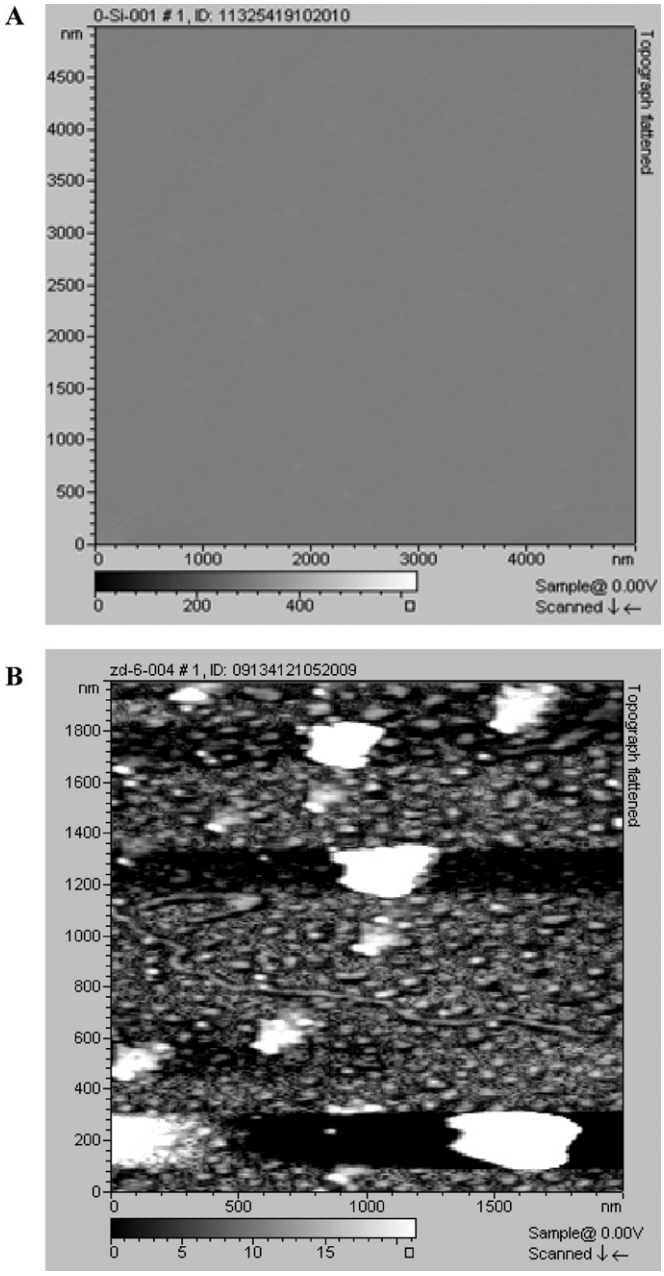

Fig. 4. AFM 2D topography images of bare silicon surface (A, scan area: 4 μm × 4 μm) and the silicon covered with a layer of DNA–ODA LB film (B, scan area: 2 μm × 2 μm).

the DNA/ODA film and access the electrode surface for exchanging electrons, because of the existence of some electrostatic repulsion between DNA and $Fe[(CN)_6]^{3-}$. This observation confirmed that DNA had been immobilized onto the electrode surface by LB techniques just as design.

3.4. Cyclic voltammetric behaviour of baicalein at DNA-LB/GCE

The flavonoid structure presents functional OH groups attached to ring structures that can be electrochemically oxidized. Fig. 6A shows the voltammograms of consecutive two cyclic scan of 5.0×10^{-7} mol L^{-1} baicalein (curves a and b) in 0.1 mol L^{-1} Britton–Robinson buffer solutions (pH = 2.87) at DNA-LB/GCE. A background voltammogram is presented as curve c in Fig. 6A. During the first cyclic scan, baicalein shows two oxidation peaks (P_1 and

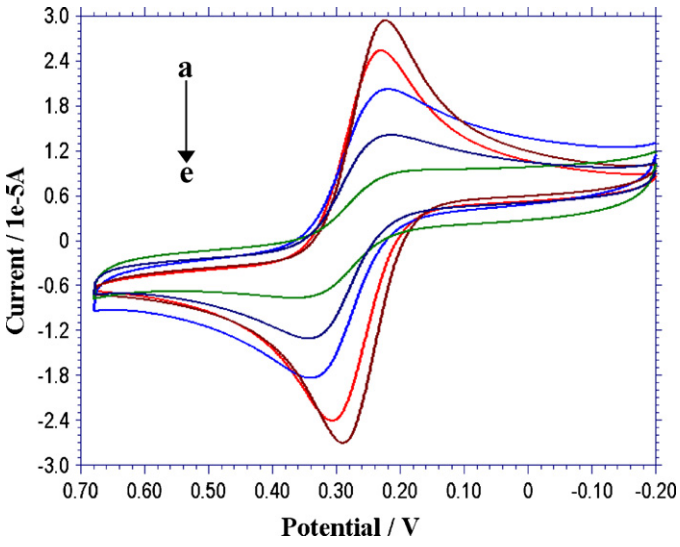

Fig. 5. Cyclic voltammograms of 2.0×10^{-3} mol L^{-1} $K_3[Fe(CN)_6]$ + 0.2 mol L^{-1} KCl solution at a clean, freshly polished bare GCE (curve a), ODA/GCE (curve b) and different layer DNA-LB/GCE (curves c–e for 1 layer, 2 layer and 3 layer) with scan rate ν = 0.10 V s^{-1}.

P_2 in curve a) with E_{pa1} = 0.463 V and E_{pa2} = 0.963 V respectively. And the two oxidation peaks disappeared almost in the second cyclic scan (curve b), which suggested a rapid and efficient passivation of the DNA-LB/GCE surface. However, if the potential was reversed before the P_2 appearance (such as at 0.8 V), this passivation phenomenon did not exist again, and a pare of redox peaks was obtained with E_{pa} = 0.463 and E_{pc} = 0.426 V (Fig. 6B, curve b). Thus, the potential scan window was controlled between 0.10 and 0.80 V in following discussion.

Fig. 7 displays electrochemical responses of 5.0×10^{-7} mol L^{-1} baicalein at bare GCE, ODA/GCE, DNA/GCE and DNA-LB/GCE, respectively. Baicalein showed electrochemical activation on all electrodes. At bare GCE, ODA/GCE and DNA/GCE, a pair of redox peaks could be discerned (Fig. 7, curves a–c). In contrast, when DNA-LB/GCE was applied, a pair of well-defined redox appeared under the same experimental condition (Fig. 7, curve d), of which the peak current is about 15-fold, 10-fold and 1.8-fold higher than that of bare GCE, ODA/GCE and DNA/GCE, respectively. This result indicated DNA-LB/GCE can greatly improve the response of baicalein. We calculate that DNA-LB/GCE has a strong affinity to baicalein, which might be partly attributed to the intercalative and electrostatic binding of the drug with the surface-confined order dsDNA layer [25,26].

To further elucidate the electrode reaction of baicalein at DNA-LB/GCE, the influence of potential scan rate (ν) on i_p of 5.0×10^{-7} mol L^{-1} baicalein was studied by CV at various sweep rates. The peak currents of baicalein grow with the increasing of scan rates and there are good linear relationships between i_p and ν, indicating the redox process of baicalein at DNA-LB/GCE was adsorption-controlled. A further evidence of the adsorption-driven reaction at the DNA-LB/GCE surface was the peak current in the second cyclic sweep decreased remarkably compared with that of the first cyclic sweep in the repetitive cyclic voltammograms. This result also confirms our explanation described above.

The influence of ν on the peak potentials of baicalein was also investigated, see Fig. 8. With the increase of ν, the oxidation peak potential was positively shifted, and the reduction peak potential was negatively shifted, indicating the redox irreversibility of baicalein was increased. These data demonstrate the electrode reaction of baicalein is a quasi-reversible process driven by adsorption. According to above results, the electron transfer kinetics of this

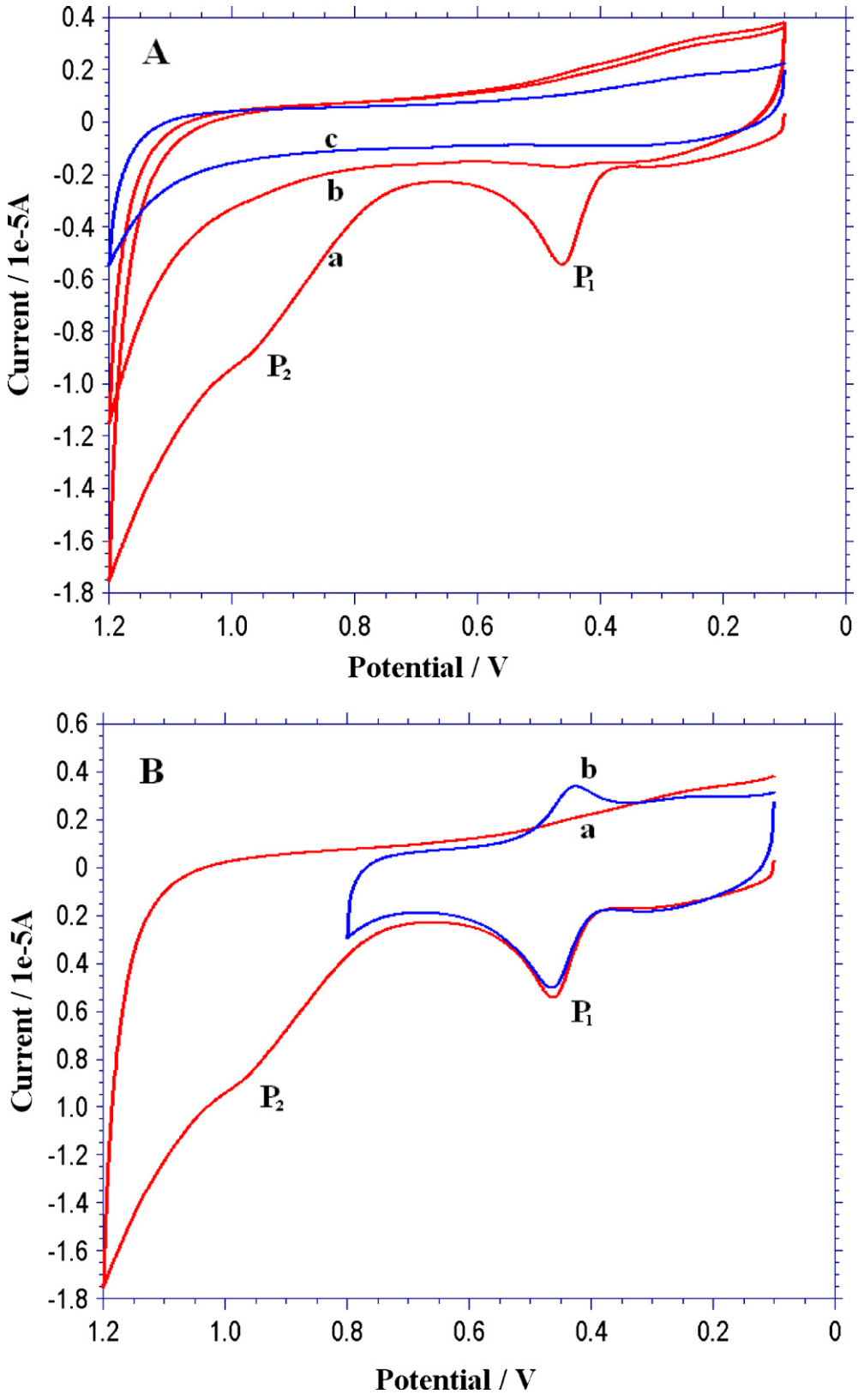

Fig. 6. (A) Cyclic voltammograms of the background (curve c) and baicalein (5.0×10^{-7} mol L^{-1}, curve a, b) in 0.1 mol L^{-1} B–R buffer solutions (pH = 2.87) at DNA-LB/GCE in the potential range of 0.10–1.20 V versus SCE. (B) Cyclic voltammograms of 5.0×10^{-7} mol L^{-1} baicalein at DNA-LB/GCE in the potential range of 0.10–1.20 V (curve a) and 0.10–0.80 V (curve b).

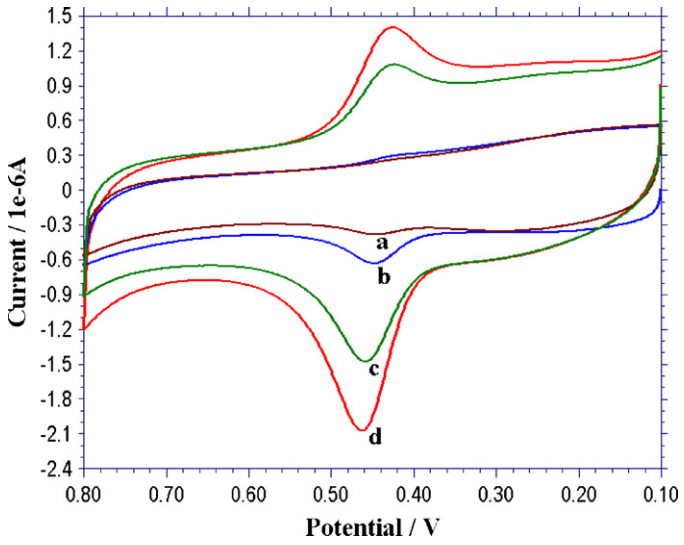

Fig. 7. Cyclic voltammograms of baicalein (5.0×10^{-7} mol L^{-1}) at bare GCE (curve a), ODA/GCE (curve b), DNA/GCE (curve c) and DNA-LB/GCE (curve d) with scan rate scan rate $\nu = 0.10$ V s^{-1}, the other experimental conditions are the same as those described in Fig. 6.

reaction system can be obtained using the approach developed by Laviron's equation [37],

$$E_{pc} = E^{0'} - \frac{RT}{\alpha nF} \ln \nu \quad (1)$$

$$E_{pa} = E^{0'} - \frac{RT}{(1-\alpha)nF} \ln \nu \quad (2)$$

$$lg\, k_s = \alpha lg\,(1-\alpha) + (1-\alpha) lg\,\alpha - lg\frac{RT}{nF\nu} - \alpha(1-\alpha)\frac{nF\Delta E_p}{2.3RT} \quad (3)$$

where $E^{0'}$ is formal standard potential; α is the charge transfer coefficient; n is the number of the electrons transferred; F is the Faraday constant (96,500 C mol^{-1}); k_s is the standard heterogeneous reaction rate constant; and ν, R and T have their usual meaning. The good linear relationships were exhibited between peak potential (E_p) and ln ν (the inset in Fig. 8) and two straight lines were gotten with two liner regression equations as E_{pa} (V) = 0.0311 ln ν + 0.468 (γ = 0.998) and E_{pc} (V) = −0.0291 ln ν + 0.369 (γ = 0.999). Then, a value of 2 could be achieved for n and α was 0.5, which was estimated from the peak width at a half-height [37]. Based on the Eq. (3), the value of appearance rate constant of electrode reaction (k_s) was further calculated to be 0.246 s^{-1}.

Next, chronocoulometriy was used to determine the saturating absorption capacity for baicalein at DNA-LB/GCE surface. The DNA-LB/GCE was immerged in a baicalein solution (5.0×10^{-5} mol L^{-1}) for several minutes to achieve saturated absorption. And then, a step potential from 0.3 V to 0.6 V was applied. $Q \sim t$ curve was recorded in Britton–Robinson solution containing 5.0×10^{-5} mol L^{-1} baicalein (Fig. 9A, curve b) to calculate the saturated absorption capacity. For control, $Q \sim t$ curve was recorded in blank Britton–Robinson solution too (Fig. 9A, curve a). The corresponding $Q \sim t^{1/2}$ plots were also performed and shown in Fig. 9B (curves a and b). As shown in Fig. 9B, the control and baicalein plots have same slope values, meaning no baicalein diffusion occurred at the electrode surface. According to the formula given by Anson [38]

$$Q = \frac{2nFAc(Dt)^{1/2}}{\pi^{1/2}} + Q_{dl} + Q_{ads} \quad (4)$$

Q_{dl} is double-layer charge; Q_{ads} is the Faradaic charge due to the oxidation of adsorbed baicalein. Using Laviron's theory of $Q = nFA\Gamma^*$ and intercepts for curves a and b, and a Γ^* value of 1.09×10^{-10} mol cm^{-2} was obtained.

3.5. Analytical applications and methods validation

3.5.1. Influence of supporting electrolyte and pH

The types of supporting electrolytes played a key role in the voltammetric responses of baicalein. The current responses of 5.0×10^{-7} mol L^{-1} baicalein were estimated in different supporting electrolytes such as a phosphate buffer, acetate buffer, Britton–Robinson and borate buffer. The results showed that higher peak current and better peak shape could be obtained

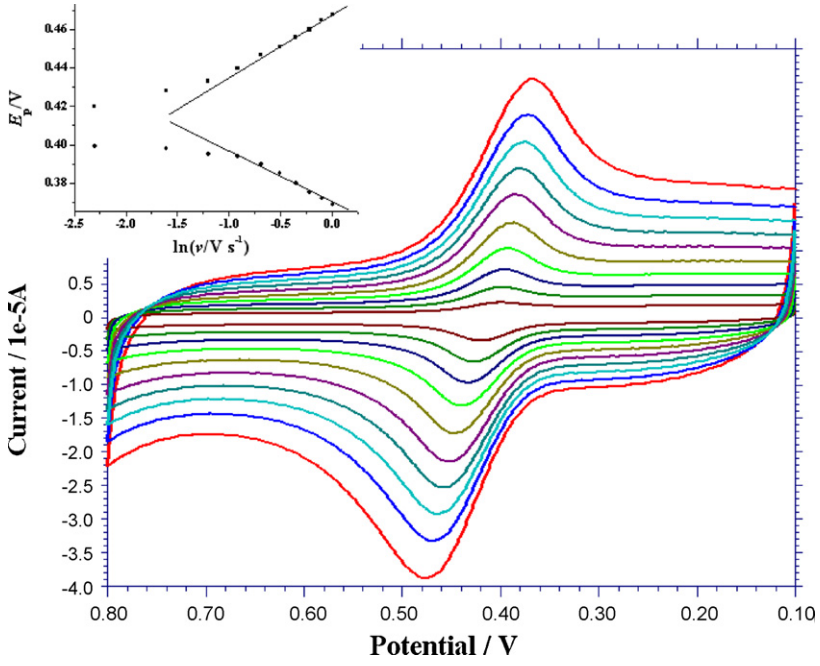

Fig. 8. CV curves of 5.0×10^{-7} mol L^{-1} baicalein at DNA-LB/GCE at different scan rate (from 1 to 10: 0.10, 0.20, 0.30, 0.40, 0.50, 0.60, 0.70, 0.80, 0.90, 1.00 V s^{-1}); insets show the relationship of the peak potential E_{pa} against ln ν, the other experimental conditions are the same as those described in Fig. 6.

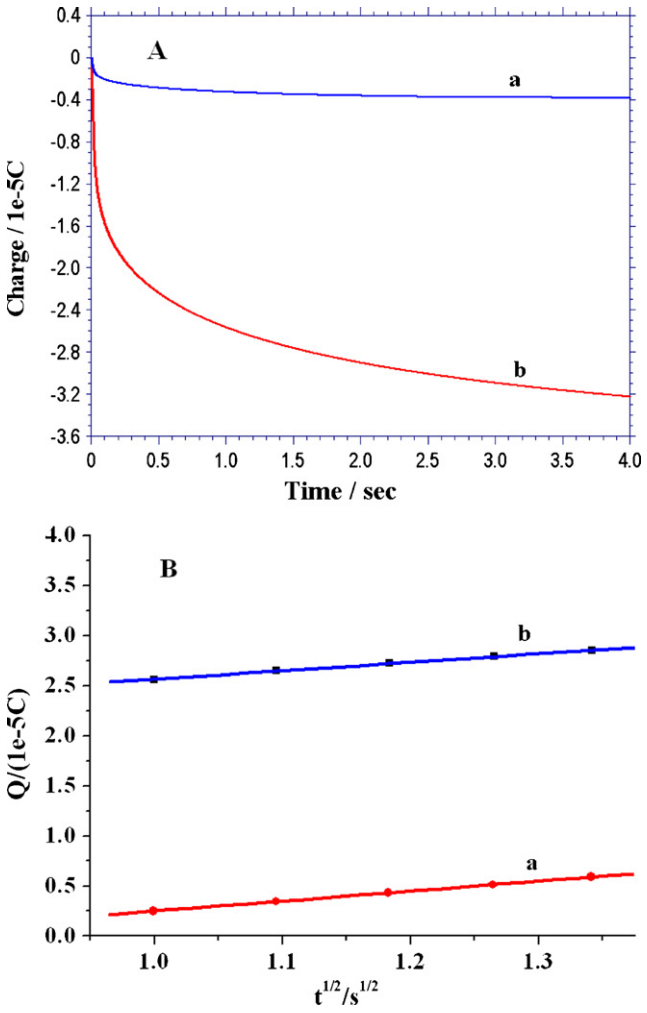

Fig. 9. (A) Chronocoulometric curves of the background (curve a) and 5.0×10^{-5} mol L^{-1} baicalein (curve b) in 0.1 mol L^{-1} B–R buffer solutions (pH = 2.87) at DNA-LB/GCE. (B) The corresponding Q–$t^{1/2}$ plots.

in Britton–Robinson buffer solution. Therefore, Britton–Robinson buffer solution was adopted.

The effect of solution pH on the formal peak potential ($E^{0'}$) was also investigated. In the pH range from 2.87 to 8.95, the value of $E^{0'}$ shifted to the negative direction with the increase of solution pH. A linear regression equation was obtained as $E^{0'}$ (V) = −0.0598pH + 0.623 (γ = 0.9988), which indicated the number of electrons and protons involved in the reaction mechanisms was the same. Thus, the electrode reaction of baicalein redox was a two-electron accompanying with two protons process. It was also found that the currents of baicalein decreased gradually with the increase of pH value. This further indicated that proton took part in the electrochemical reaction of baicalein. Therefore, pH 2.87 was chosen for the determination of baicalein.

Based on results, the electrochemical reaction mechanism was expressed as Scheme 1.

3.5.2. Influence of SWV parameters, accumulation time and potential

The SWV was used for the determination of baicalein. To obtain a much more sensitive peak current, the optimum instrumental parameters (pulse-amplitude E_{sw}, frequency f) were studied using anodic SWV for baicalein solution (5.0×10^{-7} mol L^{-1}) following accumulation time of 300 s with potential of 0.1 V. The results indicated the peak current i_p increased with the increasing of square wave amplitude from 5 to 50 mV or square wave frequency in the range of 5–50 Hz, but the peak potential shifted to more positive values and the peak changed unshapely. So a value of 35 mV was chosen as the optimum amplitude and 25 Hz were chosen as the optimum frequency.

For consideration of the adsorption of baicalein on the DNA-LB/GCE surface, SWV technique coupled with accumulation procedure was used for study. With an increase in accumulation time (t_{acc}), the peak current increased. When the t_{acc} was 180 s, peak current achieved a maximum value in a baicalein solution of 5.0×10^{-7} mol L^{-1}. A plateau was appearance for prolonging the t_{acc} afterwards. The accumulation potential had little effect on the peak current. So the t_{acc} of 180 s was used for further studies. And the accumulation of baicalein was carried out under open circuit.

3.5.3. Calibration curve, detection limit, reproducibility and stability

Fig. 10 displays the response of different baicalein concentrations under optimized working conditions using square wave adsorptive stripping voltammetry (SWASV). A linear relationship could be established between i_p and the baicalein concentrations in the range of 1.0×10^{-8}–2.0×10^{-6} mol L^{-1} (the inset of Fig. 10). The linear regression equation and correlation coefficient are:

$$i_p(\mu A) = 1.606 + 1.653 \times 10^7 C \quad (\gamma = 0.998)$$

where i_p is the reductive peak current in μA and C is the baicalein concentration in mol L^{-1}. Based on the signal-to-noise ratio of 3 (S/N), the detection limit was obtained as 6.0×10^{-9} mol L^{-1}.

The stability of the DNA-LB/GCE was checked by recording successive cyclic voltammetry. For successive 30 cycles, no change was observed of the voltammetric profiles. Using the DNA-LB/GCE to detect baicalein (5.0×10^{-7} mol L^{-1}) by SWV in pH 2.87 Britton–Robinson buffer solutions, no change was observed for 5 successive detections. Similarly, 10 different baicalein solutions (same concentration) were determined and the relative standard deviation observed was 4.2%. For testing the stability of the DNA-LB/GCE, a same baicalein solution was detected on day one and a week later. The peak currents of baicalein recorded on day one and a week later were changed about 4.4%. These experiments indicate that the DNA-LB/GCE has good stability and repeatability for the determination of baicalein.

3.5.4. Interference studies

For the possible analytical application of the proposed method, the effect of various species that likely to be in biological samples were evaluated by analysing sample solutions containing a fixed amount of baicalein (1.0×10^{-6} mol L^{-1}) spiked with various excess amount of the species under the same experimental conditions. The tolerance limit for a foreign species was taken as the largest amount yielding a relative error <±5% for the determination of baicalein. The experiment results showed that the redox peak currents of baicalein (1.0×10^{-6} mol L^{-1}) were not changed after adding 3.0×10^{-5} mol L^{-1} ascorbic acid and glucose. And 5.0×10^{-6} mol L^{-1} dopamine or epinephrine did not affect the reductive peak current of baicalein, but showed a big influence for the oxidative peak current. So the calibration curve and the content of baicalein in the commercial tablets and spiked serum samples were obtained according to the reductive peak current of baicalein. Also interference of some metal ions was tested under the same conditions. It was observed that 50-fold excess of Fe(III), Cu(II), Ca(II), Zn(II) and Mg(II) metal ions had no effects on the reductive peak. Therefore, the proposed method can be used as a selective method.

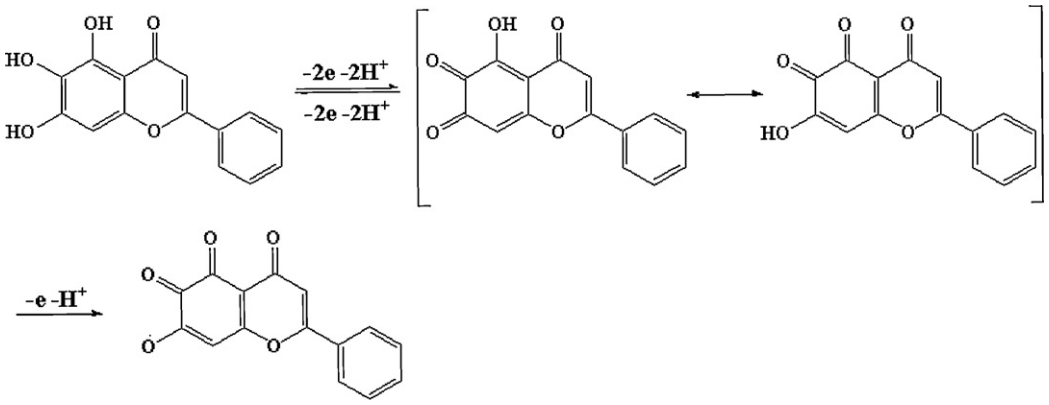

Scheme 1. Redox mechanism of baicalein at DNA-LB/GCE.

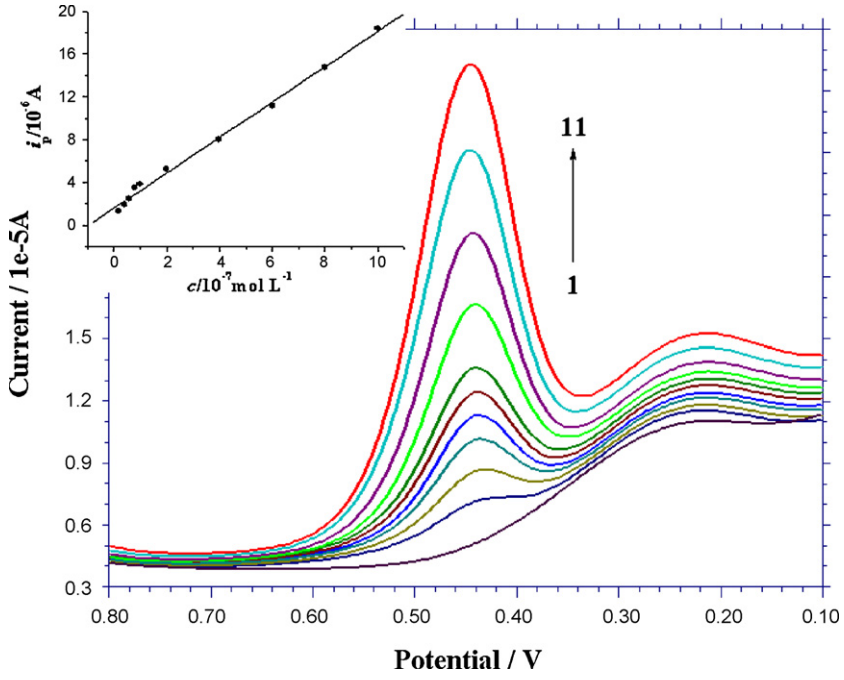

Fig. 10. Square wave anodic stripping voltammograms and their associated calibration plot (insert) for increasing concentrations of baicalein at DNA-LB/GCE under optimum conditions; baicalein concentration: (1) 0 mol L^{-1}, (2) 2.0 ×10^{-8} mol L^{-1}, (3) 4.0 × 10^{-8} mol L^{-1}, (4) 6.0 × 10^{-8} mol L^{-1}, (5) 8.0 × 10^{-8} mol L^{-1}, (6) 1.0 × 10^{-7} mol L^{-1}, (7) 2.0 × 10^{-7} mol L^{-1}, (8) 4.0 × 10^{-7} mol L^{-1}, (9) 6.0 × 10^{-7} mol L^{-1}, (10) 8.0 × 10^{-7} mol L^{-1}, (11) 1.0 × 10^{-6} mol L^{-1}.

3.5.5. Determination of baicalein in the medicinal tablets

To evaluate the practicality of the proposed method, it was employed to determine baicalein in the medicinal tablets. Five parallel samples were analyzed with relative standard deviation (RSD) of 3.4% (Table 1). After determination the content of baicalein, some standard baicalein was added in the five samples respectively and the total content of baicalein were determined again to calculate the recovery (Table 1). For testing the accuracy of proposed method, the same medicinal tablets were analyzed using HPLC method and the results were listed in Table 1 too. The contents obtained from the proposed method and HPLC method were compared using *t*-test under 95% confidence levels. The results showed that no significant difference between them. But the proposed method was simpler and more time-saving than the HPLC method.

3.5.6. Determination of baicalein in spiked serum samples

For evaluating the applicability of current method in biological samples, spiked human blood serum samples was employed for detecting baicalein. No baicalein signal was observed in direct determination and then, some standard baicalein was added in sample for testing the recovery. The results of determination are listed in Table 2. The mean recovery of baicalein was 99.0%.

Table 1
Determination results of baicalein in the medicinal tablets by SWASV and HPLC.

SWASV (n = 5)					HPLC (n = 3)	
Amount found (mg L^{-1})	R.S.D. (%)	Standard added (mg L^{-1})	Total found (mg L^{-1})	Recovery (%)	Amount found (mg L^{-1})	R.S.D. (%)
2.012	3.4	2.0	3.946	96.7	2.103	2.1

Table 2
Application of the SWASV method to the determination of baicalein in spiked human blood serum samples.

Sample	Original found (1.0×10^{-7} mol L^{-1})	Added (1.0×10^{-7} mol L^{-1})	Total found[b] (1.0×10^{-7} mol L^{-1})	R.S.D. (%)	Recovery (%)
1	ND[a]	2.00	1.89	3.1	94.5
2	ND[a]	4.00	4.21	4.0	105.3
3	ND[a]	6.00	5.91	2.7	98.5
4	ND[a]	8.00	7.82	3.2	97.8

[a] ND, none detected.
[b] Average of three determinations.

4. Conclusion

In current work, we designed a highly sensitive electrochemical sensor, based on DNA LB film modified electrode, for the detection of trace amounts of baicalein. The existence of DNA LB film on the electrode surface remarkably improved the response of baicalein. The adsorptive voltammetric behaviours of baicalein on DNA-LB/GCE were explored by CV and SWV. By using the DNA-LB/GCE, trace amounts of baicalein could be detected with LOD of 6.0×10^{-9} mol L^{-1} by SWASV under accumulation time of 180 s. The proposed method was also applied for the determination of baicalein in the medicinal tablets and spiked human blood serum samples. This research suggests that designed and modified electrode with LB techniques of DNA might be a very promising basis for analytical sensing. The arm of this work is to provide a new avenue for electrochemical investigation of baicalein in biochemical, pharmaceutical and clinical research.

Acknowledgements

The authors gratefully acknowledge the financial support of the National Natural Science Foundation of China (No. 20775073), the Natural Science Foundation of Henan Province in China (Nos. 2008A150008, 2010B150007) and Postgraduate Scientific Research Foundation of Zhengzhou University (No. 10L00304).

References

[1] C.S. Yang, J.M. Landau, M.T. Huang, H.L. Newmark, Annu. Rev. Nutr. (2001) 381–406.
[2] D. Yang, H. Hu, S. Huang, J.P. Chaumont, J. Millet, Zhong Yao Cai 23 (2000) 272–274.
[3] T. Nakajima, M. Imanishi, K. Yamamoto, J.C. Cyong, K. Hirai, Planta Med. 67 (2001) 132–135.
[4] K. Kitamura, M. Honda, H. Yoshizaki, S. Yamamoto, H. Nakane, M. Fukushima, K. Ono, T. Tokunaga, Antiviral Res. 37 (1998) 131–140.
[5] F.L. Chan, H.L. Choi, Z.Y. Chen, P.S.F. Chan, Y. Huang, Cancer Lett. 160 (2000) 219–228.
[6] S. Ikemoto, K. Sugimura, N. Yoshida, R. Yasumoto, S. Wada, K. Yamamoto, T. Kishimoto, Urology 55 (2000) 951–955.
[7] M. Li-Weber, Cancer Treat. Rev. 35 (2009) 57–68.
[8] Y. Matsuzaki, N. Kurokawa, S. Terai, Y. Matsumura, N. Kobayashi, K. Okita, Jpn. J. Cancer Res. 87 (1996) 170–177.
[9] D.E. Shieh, L.T. Liu, C.C. Lin, Anticancer Res. 20 (2000) 2861–2865.
[10] Z.H. Gao, K.X. Huang, X.L. Yang, H.B. Xu, Biochim. Biophys. Acta – Gen. Subj. 1472 (1999) 643–650.
[11] Y.F. Du, J. Zhou, B.H. Yao, Chem. Anal. Meterage 17 (2008) 43–45.
[12] B. Li, L. Guo, C. Xu, L. Ma, Spectrochim. Acta A: Mol. Biomol. Spectrosc. 71 (2008) 892–897.
[13] M. Okamoto, M. Ohta, H. Kakamu, T. Omori, Chromatographia 35 (1993) 281–284.
[14] L. Zhang, L. Xu, X.J. Tan, Q.F. Liao, W. Guo, X.H. Chen, K.S. Bi, Chromatographia 66 (2007) 115–120.
[15] L. Zhang, G. Lin, Z. Zuo, J. Pharm. Biomed. Anal. 36 (2004) 637–641.
[16] Y. Peng, X. Ding, Q. Chu, J. Ye, Anal. Lett. 36 (2003) 2793–2803.
[17] G. Chen, H. Zhang, J. Ye, Talanta 53 (2000) 471–479.
[18] M. Fojta, T. Kubiárová, E. Paleek, Electroanalysis 11 (1999) 1005–1012.
[19] S. Palanti, G. Marrazza, M. Mascini, Anal. Lett. 29 (1996) 2309–2331.
[20] K.M. Millan, S.R. Mikkelsen, Anal. Chem. 65 (1993) 2317–2323.
[21] G. Marrazza, I. Chianella, M. Mascini, Biosens. Bioelectron. 14 (1999) 43–51.
[22] F. Patolsky, E. Katz, A. Bardea, I. Willner, Langmuir 15 (1999) 3703–3706.
[23] J. Wang, X. Cai, G. Rivas, H. Shiraishi, P.A.M. Farias, N. Dontha, Anal. Chem. 68 (1996) 2629–2634.
[24] P. Palaska, E. Aritzoglou, S. Girousi, Talanta 72 (2007) 1199–1206.
[25] F. Wang, Y.J. Wu, L. Gao, T.L. Xing, B.X. Ye, Electroanalysis 21 (2009) 1692–1698.
[26] F. Wang, Y.J. Wu, J.X. Liu, B.X. Ye, Electrochim. Acta 54 (2009) 1408–1413.
[27] Z.S. Yang, J. Zhao, D.P. Zhang, Y.C. Liu, Anal. Sci. 23 (2007) 569–572.
[28] J. Zhao, G.Z. Hu, Z.S. Yang, Y.Y. Zhou, Anal. Lett. 40 (2007) 459–470.
[29] E. Palecek, M. Fojta, Anal. Chem. 66 (1994) 1566–1571.
[30] K. Hashimoto, K. Ito, Y. Ishimori, Anal. Chem. 66 (1994) 3830–3833.
[31] G.G. Roberts, Langmuir Blodgett Films, Plenum, New York, 1990.
[32] E. Guaus, J. Torrent-Burgues, N. Zine, A. Errachid, Sensor Lett. 7 (2009) 1006–1011.
[33] W. Chen, J.M. Kim, L.P. Xu, S.H. Sun, S.W. Chen, J. Phys. Chem. C 111 (2007) 13452–13459.
[34] M. Ferreira, L.R. Dinelli, K. Wohnrath, A.A. Batista, O.N. Oliveira, Thin Solid Films 446 (2004) 301–306.
[35] H.S. Wang, H.X. Ju, H.Y. Chen, Electroanalysis 13 (2001) 1105–1109.
[36] S.X. Dai, X.T. Zhang, Z.L. Du, H.X. Dang, Mater. Lett. 59 (2005) 423–429.
[37] E. Laviron, J. Electroanal. Chem. 101 (1979) 19–28.
[38] F.C. Anson, Anal. Chem. 36 (1964) 932–934.